Austin Journal of Biomedical Engineering

Open Access

Austin Publishing Group

Research Article

# Enhancing Cancer Radiation Therapy with Cell Penetrating Peptide Modified Gold Nanoparticles

**Send Kah Ng[1], Liyuan Ma[1], Yuting Qiu[1], Xiaojie Xun[2], Thomas J. Webster[1,2,3] and Ming Su[1,2]***

[1]Department of Chemical Engineering, Northeastern University, Boston, Massachusetts, USA

[2]Wenzhou Institute of Biomaterials and Engineering, Chinese Academy of Sciences, Wenzhou, Zhejiang, China

[3]Center of Excellence for Advanced Materials Research, King Abdulaziz University, Jeddah, Saudi Arabia

***Corresponding author:** Ming Su, Department of Chemical Engineering, Northeastern University, USA

**Received:** April 20, 2016; **Accepted:** June 22, 2016; **Published:** June 24, 2016

**Abstract**

Radiotherapy is one of the most prevalent methods for cancer treatment. However, a challenge for cancer radiotherapy is that therapeutic doses used can damage neighboring normal cells. This paper describes a new method to enhance radiation therapy by delivering gold nanoparticles into cancer cells, where gold nanoparticles were modified with virus-derived cell penetrating peptides (CPPs) and Poly (Ethylene Glycol) (PEG). PEG was used to improve nanoparticles blood circulation time, and CPPs were used to enhance internalization of the nanoparticles into cells. The internalization of CPP-PEG modified gold nanoparticles in cancer cells (HeLa cells) was confirmed with differential interference contrast imaging. A variety of assays (such as bright field imaging, MTT, DNA damage, reactive oxygen species and immunofluorescence) were used to detect cellular and genetic damage in cancer cells. We found that CPP-PEG modified gold nanoparticles caused more cellular and DNA damage than gold nanoparticles at the same radiation doses due to enhanced generation of free radicals. In contrast, damage was not severe for normal fibroblasts cells under the same conditions. This method can potentially be used to severely damage DNA and other cellular structures of cancer cells, while minimizing damage to normal cells during radiation therapy.

**Keywords:** cell penetrating peptides; gold nanoparticles; radiation therapy

## Introduction

Currently, chemotherapy, surgery and radiotherapy are the most effective methods to treat cancer [1]. Radiotherapy targets and destroys tumor with ionizing radiation. The laser generates free radicals that damage various cellular components including DNA. One of the advantages of using radiotherapy is that it can kill tumor even though they are intermix with normal healthy tissue [2]. Hence, more than 50% of cancer patients received radiotherapy treatment. However, the therapeutic doses used during radiotherapy can damage nearby normal cells [3-5]. Various chemicals and nanoparticles were tested to act as radiosensitlzers to enhance radiotherapy [6].

Despite its essential role in maintaining cell function, cell membranes present a major barrier for intra-cellular delivery of therapeutic nanoparticles [7]. Hence, even though ions or nanoparticles of high atomic number elements (such as gold, platinum and bismuth) have been used to enhance radiation therapy by absorbing ionizing radiation and generating free radicals at high yield [8-10], the measured enhancement effect due to nanoparticles has been negligible, likely because inefficient nanoparticles were present in cancer cells and X-ray generated free radicals cannot reach the vicinity of DNA to cause damage [11,12].

Nanoparticles can be modified to have desirable surface properties to allow for uptake and targeted delivery into cells and sub-cellular locations [13,14]. Non-viral vectors such as amino-modified silica nanoparticles, iron oxide nanoparticles, carbon nanotubes and gold nanoparticles have been used to deliver nucleic acids in transfection assays [15-18]. In particular, gold (Au) nanoparticles are stable, non-toxic and easy for surface modification, making them a suitable candidate to deliver molecules into cells [19-23]. However, to reach their full potential in cellular applications such as radiotherapy, robust methods must be developed to allow for the controlled uptake of gold nanoparticles into cells. This requires the gold nanoparticles to be functionalized with engineered coatings to promote their cellular uptake and targeted delivery.

Poly ethylene glycol (PEG) was used to coat nanoparticles to improve their blood circulation [24]. However, PEG interactions with cell surface ligands prevent nanoparticles intra-cellular uptake. One solution to use cell penetrating peptides (CPPs). CPPs are relatively short cationic and/or amphipathic peptides and are efficient cellular delivery vectors due to their intrinsic ability to enter cells and mediate uptake of a wide range of macromolecular cargo [25]. The various molecular cargo delivered by CPPs ranges from nanosize particles to small chemical molecules and large fragments of DNA. The "cargo" is associated with the peptides either through chemical linkage via covalent bonds or through non-covalent interactions [26]. The function of the CPPs is to deliver the cargo into cells, a process that commonly occurs through endocytosis with the cargo delivered to the endosomes of living mammalian cells [27,28].

In our study, coating of gold nanoparticles with PEG prevents the gold nanoparticles from aggregation and allows the nanoparticles to evade immunological response *in vivo* [29]. This gives the nanoparticles a longer circulation time in the body and increases their chance to accumulate inside the cancer cells. The CPPs with multiple arginine residues and positively charged motif derived from human immunodeficiency virus (HIV) Transcriptional Activator Protein




**Citation:** Seng Kah Ng, Liyuan Ma, Yuting Qiu, Xiaojie Xun, Thomas J, Webster, et al. Enhancing Cancer Radiation Therapy with Cell Penetrating Peptide Modified Gold Nanoparticles. Austin J Biomed Eng. 2016; 3(1): 1033.

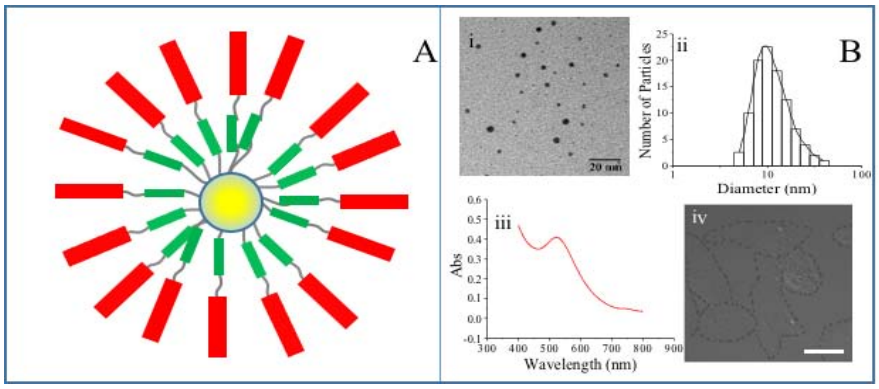


**Figure 1:** Enhanced radiation therapy with cell penetrating peptide modified gold nanoparticles. (A) Schematic diagram of gold nanoparticles (gold) modified with PEG (green) and CPP (red). (B) TEM image of gold nanoparticles (i), scale bar is 20 μm; size distribution (ii) and UV-vis absorption spectrum of nanoparticles (iii) of 10 nm PEG-CPP-AU modified nanoparticles; optical image of internalized PEG-CPP-AU nanoparticles into HeLa cells (i), scale bar is 10 μm.

(Tat), has been shown to mediate the endocytic uptake of a number of different nanoparticles in eukaryotic cells [30].

This paper describes a new method to enhance X-ray radiation killing of cancer cells by internalizing CPP-PEG modified gold nanoparticles (as radiosensitizers) into cells (Figure 1A). We hypothesized that at a given irradiation dosage, if gold nanoparticles could be placed specifically inside cancer cells and close to cell nuclei, more free radicals would be available to cause DNA damage. Hence, the total radiation dose could be reduced to receive the same treatment effect on cancer cells without severely damaging the healthy cells nearby.

## Methods and Materials

### Gold nanoparticle modification

A $HAuCl_4.3H_2O$ stock solution was made by mixing 100 mg of $AuCl_4$ in 5 ml of distilled water. 72 μl of an 880 mM sodium borohydride ($NaBH_4$) stock solution in deionized water was then added over 30 min with vigorous stirring. To make the gold nanoparticles, 156 μL of a 50.8 mM $HAuCl_4.3H_2O$ stock solution and 169 μM of a SH-PEG-COOH (molecular weight 3.4 k, Creative PEG Works) solution were dissolved in 25 ml of deionized water and stirred at room temperature for 1 hour. After the addition of $NaBH_4$, the mixture was left stirring for 3 hours. Extra SH-PEG-COOH and $NaBH_4$ were added to ensure the passivation of the nanoparticles. Gold nanoparticles were thiol linked to the PEG. To make gold nanoparticle-PEG-CPP conjugates, PEG-COOH modified gold nanoparticles (2 mM) were mixed with CPP with a sequence of WGRRVRRRIRRPPPPPPPPPGGK at a 400:1 (CPP/nanoparticle) ratio with 150 mM EDC and 7.5 mM sulfo-NHS (final concentration) in a 1 ml total reaction volume for 2 hours at room temperature.

### Cell culture with modified gold nanoparticles

HeLa (CLL-2) and human fibroblasts (CCL-110) cell lines were obtained from the American Type Culture Collection (ATCC). Cells were cultured in a tissue culture flask (Thermo Scientific) in an incubator at 37 °C in an atmosphere of 5% $CO_2$ with DMEM medium (Bio Whittaker) that is supplemented with 10% serum, 1% penicillin-streptomycin (Sigma-Aldrich) and 2 mM glutamine (Life Technologies). Cells were seeded in a 96-well micro plate at a concentration of 5,000 cells per well. After 24 hours, CPP modified gold nanoparticles were incubated with cells at a final concentration of 2, 10, 20, 50 and 100 μM, respectively. Excess nanoparticles in the medium were removed after incubation for 24 hours. Cells grown in 75 $cm^2$ culture flasks with respective concentrations of nanoparticles were imaged at 24, 48 and 72 hours with or without X-ray using an IX71 Olympus microscope and Hamamatsu digital camera. A Mini-X portable X-ray tube (Amptek, Bedford, MA) with a silver anode operating at 40 kV and 100 mA is used to generate primary X-rays and irradiate cells at a distance of 5 cm for 15 minutes for all X-ray irradiation experiments.

### Cell proliferation assay

Cells were grown in 96 well plates (Corning) at approximately 70% cell confluence. Gold nanoparticles at various concentrations (0.5, 1, 2, 10, 20, 50, 100, 250, 500 and 1000 μM) were added into the cell culture media in triplicate to calculate $IC_{50}$ values. Cells were irradiated with an X-ray (40 kVp and 100 μA) at the next day for 15 minutes. After incubation for 24 hours, a Vybrant MTT cell proliferation assay (Life Technologies) was performed. Absorbance was measured according to vendor instructions using a Spectra Max M3 plate reader (Molecular Devices). Two independent sets of experiments were performed.

### Reactive oxygen species (ROS) production

Carboxy-H2DCFDA was used to measure ROS production from X-ray irradiation. In the presence of ROS, carboxy-H2DCFDA was oxidized and emitted green fluorescence. Carboxy-H2DCFDA was added at a final concentration of 1 μM into the wells of 96 well microplates. Gold nanoparticles were added at a concentration of 2, 10, 20, 50 and 100 μM a day prior to the experiment. The microplates were incubated in the dark for 30 minutes. The medium containing carboxy-H2DCFDA was removed and washed twice with phosphate-buffered saline (PBS). After adding fresh medium, cells were immediately irradiated with an X-ray for 15 minutes, followed by incubation for one hour. The fluorescence intensity at 527 nm was measured using a fluorescence plate reader using 492 nm excitation, respectively. Two independent experiment sets were performed. The distribution of ROS after X-ray irradiation was imaged as follows: the cells were cultured in coverslips, exposed to X-ray radiation, treated with reagent, fixed by 4% paraformaldehyde for 10 minutes, washed with PBS, and mounted onto glass slides.

### DNA damage observation

A day after cells were incubated with gold nanoparticles in a 25 $cm^2$ tissue culture flask, cells were exposed to an X-ray, trypsinized after 24 hours, and re-plated onto a 6 well culture dish with sterilized coverslips at the bottom of each well. Once cells attached to coverslips, cells were mounted on a glass slide using mounting medium vetashield (Vector) containing DAPI (4',6-diamidino-2-phenylindole). DAPI is a fluorophore that can be used to visualize nuclei content by binding strongly to adenine-thymine rich regions in DNA. If there was any serious DNA damage, the change in nuclei morphology would be observed through DAPI staining. The samples were visualized using a confocal microscope (ZEISS), and more than 60 cells were counted to determine if their DNAs were damaged.

### Immunofluorescence

Immunostaining of X-ray irradiated cells was performed as follows. Cells were cultured on coverslips in 6 wells plates and exposed to an X-ray for 15 minutes. One day after irradiation, the cells were fixed by 4% paraformaldehyde for 10 minutes, washed with a wash buffer (0.2% Triton-X 100 in PBS) for three times and incubated with a blocking buffer (1% BSA, and 0.2% Triton-X 100 in PBS) for 1 hour at room temperature. Primary antibodies for anti-phospho-histone H2AX (pSer139) (Sigma, 1:500) were incubated overnight in a blocking buffer at 4°C.The next day, cover slips were washed three times in a wash buffer, and a rabbit secondary antibody (In vitrogen, 1:2000) was added for 2 hours at room temperature. The cover slips were rinsed three times in wash buffer before mounting on glass slides. A laser confocal microscope (Zeiss) with a 20 X magnification was used to collect all images.

### Differential interference contrast (DIC) microscopy

Differential interference contrast (DIC) microscopy was used to determine the location of gold nanoparticles inside cells as follows. The TPMT image setting on Zen software was selected and a DIC III filter with a light polarizer was in place to obtain the DIC effect. For Z-sectioning DIC images, maximum projections of 15 images of *z*-planes 1 μm apart were taken and merged into one image. DIC images were taken at a 60X magnification. All images were digitally processed with Adobe PhotoShop CC 2014 (Adobe Systems Inc., Mountain View, CA).

### Apoptosis study

HeLa cells were treated with modified gold nanoparticles and stained with Annexin V–FITC and PI and evaluated for apoptosis by flow cytometry according to a FITC Annexin V apoptosis detection kit per manufacturer's protocol (BD Phar Mingen). Briefly, approximately 100,000 cells were washed twice with ice cold PBS, and stained with 5 μL of Annexin V–FITC and 5 μL of PI in a binding buffer (10 mM HEPES, pH 7.4, 140 mM NaOH, 2.5 mM $CaCl_2$) for 15 mins at room temperature in the dark. Apoptotic cells were determined using a Becton-Dickinson FAC Scan cytoflurometer (Mansfield, MA, USA). Both early apoptotic (annexin V-positive, PI-negative) and late (annexin V-positive and PI-positive) apoptotic cells were included in the calculation.

### Statistical analysis

Each experiment was repeated three times, and student's t-tests were used to determine statistical significance. $P < 0.05$ was considered to be statically significant. Results were presented as mean ± S.E.M. $IC_{50}$ values were calculated using logarithmic equations.

## Results and Discussion

### Gold nanoparticle characterization

Several techniques were used to characterize gold nanoparticles. The size of gold nanoparticles was characterized with transmission electron microscopy (TEM) using a JEOL 1011 TEM operated at 100 kV. Figure 1Bi is a TEM image of gold nanoparticles, where spherical nanoparticles with diameter of 8 nm can be seen. The hydrodynamic diameter and surface charges of nanoparticles were examined with dynamic light scattering (DLS) using Zetasizer Nano-ZSP (Malvern Instruments Ltd., UK). A fixed nanoparticle concentration of 50 nM was used to ensure reproducibility of measurements which is showed in Figure 1Bii. For zeta potential measurements, a constant voltage of 150 mV was applied. Gold nanoparticles had a hydrodynamic diameter of 12±3.4 nm and zeta potential of 3.8 mV. UV-vis measurement was performed on a Cary 4000 UV-Vis spectrophotometer (Varian Inc., CA, USA). Figure 1Biii is the UV-vis absorption spectrum of nanoparticles, where the adsorption peak at 522 nm indicates the extinction peak of gold nanoparticles.

### Internalization of PEG-CPP modified gold nanoparticles

To determine if there was internalization of PEG-CPP-Au nanoparticles into cells, PEG-CPP-Au nanoparticles were incubated with HeLa cells overnight with PEG-CPP modified gold nanoparticles, and fixed with 4% paraformaldehyde the following day. The cells were washed with PBS, then mounted onto slides and imaged with confocal microscope using DIC settings. Figure 1Biv showed that all cells incubated with PEG-CPP modified gold nanoparticles contained vesicles internally, while most of the untreated cells did not have or contained only a few of these vesicles (not shown). Z-sectioning of the samples was carried out to detect all the potential vesicles that were present in the cells, and the images were merged together using maximum projection setting. The maximum projection images (not shown) indicated that cells incubated with PEG-CPP modified gold nanoparticles contained a large amount of nanoparticles inside the cells. For untreated cells, the small number of nanoparticles present intra-cellularly might be vacuoles involved in normal metabolic activities (not shown).

### Cytotoxicity of PEG-CPP modified gold nanoparticles

Cytotoxicity of nanoparticles tested *in vitro* by visual inspection of the cells with bright-field microscopy for changes in cellular morphology over a time period. Figure 2A showed HeLa cells treated with 20 μM of gold nanoparticles, PEG modified gold nanoparticles, and PEG-CPP modified gold nanoparticles. Figure 2Aiii showed that a large amount of cells treated with PEG-CPP modified nanoparticles that underwent irradiation changed morphology, and became elongated with a shriveled up appearance 48 hours later. In comparison, in the absence of an X-ray, there was no morphological change in most cells after incubation with PEG-CPP gold nanoparticles for 48 hours (Figure 2Biii).

The viability of the cells treated with gold nanoparticles, PEG modified gold nanoparticles, and PEG-CPP modified gold nanoparticles were monitored with MTT assays. As a comparison, the cytotoxicity of CPP or unmodified gold nanoparticles with free

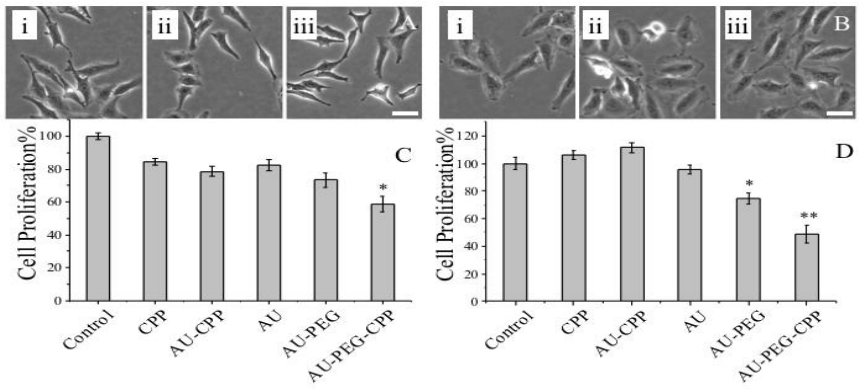


**Figure 2:** Cytotoxicity of gold nanoparticles modified with PEG-CPP. HeLa cells treated with gold nanoparticles (i) PEG modified gold nanoparticles and (ii) PEG-CPP modified gold nanoparticles (iii) with (A) or without (B) X-ray irradiation. Figures showing the percentage of cells relative to the untreated control cells after incubating with nanoparticles 24 hours after X-ray irradiation (C) or without X-ray irradiation (D). For Figure 2C, the number of cells for all the treatments were compared to X-ray irradiated cells. For figure 2D, the number of cells was compared to cells that were not X-ray irradiated. Scale bar is 20 μm. *, $P < 0.005$, **, $P < 0.001$.

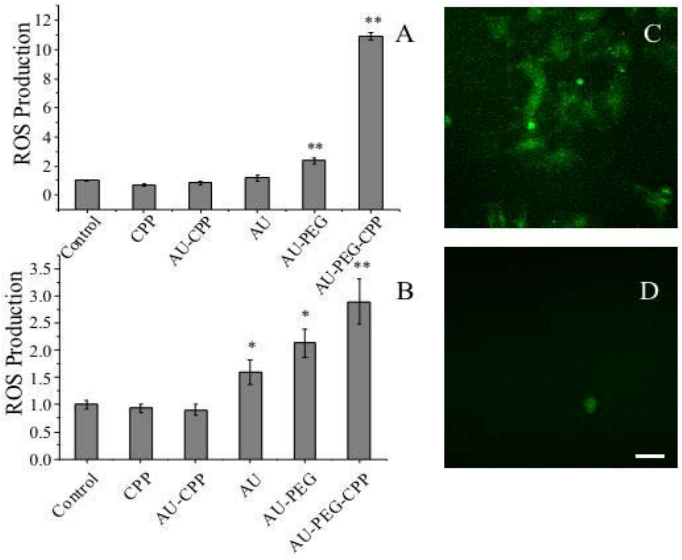


**Figure 3:** Reactive oxygen species (ROS) production after HeLa cell X-ray irradiation. The relative amount of ROS produced compared to controls using carboxy-$H_2$DCFDA assays after treated with different nanoparticles with X-ray (A) or without (B) X-ray irradiation. Fluorescence images showing levels of ROS produced when cells were treated with PEG-CPP modified gold nanoparticles (C) or gold nanoparticles (D) and underwent X-ray irradiation. For Figure 3A, the number of cells for all the treatments were compared to X-ray irradiated cells. For Figure 3B, the number of cells was compared to cells that were not X-ray irradiated. Scale bar is 20 μm. *, $P < 0.005$, **, $P < 0.001$.

CPP was tested. With X-ray irradiation, 58.8% of the cells treated with PEG-CPP gold nanoparticles died a day later as compared to untreated cells (Figure 2C). The survival rates from other treatments ranged from 84 to 73%. Without irradiation, 48.7% of cells treated with PEG-CPP gold nanoparticles died as compared to the untreated cells, while the survival rate from other treatments did not vary too much except those treated with PEG modified gold nanoparticles which had a survival rate of 74.3% (Figure 2D). Taken together, 20 μM of PEG-CPP modified gold nanoparticles exhibited a more cytotoxicity effect on HeLa cells after X-ray irradiation as compared to other gold nanoparticle modifications.

## ROS production upon X-ray irradiation

Ionizing X-ray radiation causes water radiolysis, generating intra-cellular reactive oxygen species (ROS) [31-34]. ROS can cause oxidation damage to DNA, resulting in single or double DNA strand breakage and giving rise to genomic instability [35,36]. To determine if PEG-CPP modified gold nanoparticles can enhance ROS production after X-ray irradiation (40 kV, 100 mA), HeLa cells were incubated overnight with various modified gold nanoparticles. An 11 fold increase in ROS production was observed when cells treated with PEG-CPP modified gold nanoparticles were exposed to X-ray radiation, as compared to untreated cells (Figure 3A). In contrast, without X-ray irradiation, there was only three fold increase in ROS production when cells were treated with PEG-CPP modified gold nanoparticles (Figure 3B). The ROS yields in cells that were treated with other gold nanoparticle modifications were not as significant as

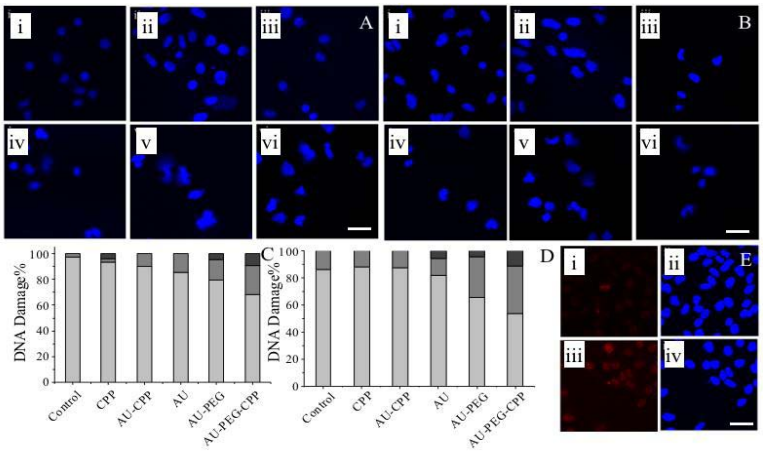


**Figure 4:** HeLa cells treated with various nanoparticles at 20 μM concentrations and stained with DAPI with X-ray (A) or without (B) X-ray irradiation. Control (i), CPP (ii), Au nanoparticles with free CPP (iii), Au nanoparticles (iv), PEG-Au nanoparticles (v) and PEG-CPP-Au nanoparticles (vi). Measurements of DNA damage 2 days after nanoparticle incubation with (C) and without (D) X-ray irradiation (Light grey bar: No DNA damage, Grey bar: Moderate DNA damage, Dark grey bar: Severe DNA damage). Immuno-fluorescence images of X-ray irradiated cells treated with either gold nanoparticles (i) or gold nanoparticles modified with PEG-CPP (ii) and probed with antibodies against anti-phoso-histone H2AX (pSer139) (E). Scale bar is 20 μm.

that of PEG-CPP modified ones. To visualize ROS production, cells were fixed and mounted on slides 1 hour after X-ray irradiation, and images were taken using a confocal microscope. Figure 3C shows a higher level of ROS production (green fluorescence) when cells that were treated with PEG-CPP gold nanoparticles were irradiated, compared to cells containing only gold nanoparticles (Figure 3D). As compared to other types of nanoparticles, PEG-CPP modified gold nanoparticles significantly enhanced ROS production after irradiation when they were internalized in the cells (Figure 1B).

## DNA damage upon X-ray irradiation

H2AX protein level is up-regulated when there is insult to DNA integrity [37-39]. High levels of phosphorylation on Ser-139 of H2AX is linked to cell death after DNA damage [40]. ROS induction is partly mediated by increasing H2AX levels [41]. Thus, understanding the correlation of DNA damage with levels of H2AX phosphorylation after X-ray irradiation is crucial to determine cell fate after DNA damage. X-ray irradiated HeLa cells were stained with DAPI and images were taken using confocal microscopy to determine the level of damage to DNA. Figure 4A (v and iv) shows a larger number of nuclei of cells treated with PEG gold nanoparticles and PEG-CPP modified gold nanoparticles appeared damaged with a distorted nuclei structure, compared to other treatments. To determine the proportion of damaged nuclei, at least 60 nuclei were counted from each group and the results were tabulated on Figure 4C. 46% and 35% of irradiated nuclei were damaged when treated with PEG-CPP modified gold nanoparticles or PEG modified gold nanoparticles, respectively; while 13% of nuclei from cells without nanoparticles were damaged (Figure 4C). Figure 4D showed that in the absence of radiation, 31% and 19% of nuclei were damaged when treated with PEG-CPP modified gold nanoparticles or PEG modified gold nanoparticles, respectively; while 2% of nuclei from cells without nanoparticles were damaged.

To determine if H2AX protein was phosphorylated on Ser-139 upon exposure to X-ray irradiation and PEG-CPP modified gold nanoparticles, HeLa cells treated with either gold or PEG-CPP modified gold nanoparticles were irradiated. Cells were fixed one day later, and tested with primary antibodies against anti-phoso-histone H2AX (pSer139). The following day, after the samples were probed with a secondary antibody tagged with Texas red flurophore and stained with DAPI, cells were mounted onto slides to take fluorescence images. Figure 4Eiii shows a higher expression of phosphorylated H2AX specifically in the irradiated nuclei when cells were treated with PEG-CPP modified gold nanoparticles as compared to gold nanoparticle treatments. Thus, cells treated with PEG-CPP modified gold nanoparticles and X-ray irradiation suffered from a higher rate of DNA damage, and more H2AX protein was phosphorylated.

## Flow cytometry for cell viability examination

Extensive DNA damage can lead to either cell apoptosis or cell death [42-44]. Flow cytometry was used to determine if cell death caused by X-ray irradiation and PEG-CPP modified gold nanoparticles was mainly due to cells undergoing apoptosis or necrosis. 20 μM of PEG-CPP modified gold nanoparticles were incubated with HeLa cells and irradiated with an X-ray. The following day, the cells were analyzed using flow cytometry using annexin V/PI double staining. 36.53% of cell death was observed (Figure 5B and D). Out of these dying cells, ~60 % were caused by early or late apoptosis (Figure 5B, upper and lower left quadrants and 5D). In contrast, 12.14% of irradiated cells were dying, and ~40 % of these cells died by apoptosis (Figure 5A, upper and lower left quadrants and 5D). Figure 5C indicated a higher proportion of PEG-CPP modified gold nanoparticles treated cells with apoptosis marker Annexin V staining (green line) as compared to the control (blue curve). Hence, the majority of HeLa cells died by apoptosis when treated with both X-ray irradiation and PEG-CPP modified gold nanoparticles.

## Nanoparticle concentration effect on cell death

Nanoparticles toxicity has been shown to function in a concentration-dependent manner. Hence, determination of an appropriate nanoparticle dose to utilize in a cytotoxicity assay is key to understanding the toxic effects of the nanoparticles. We performed concentration-dependent cytotoxicity of nanoparticles as follows.

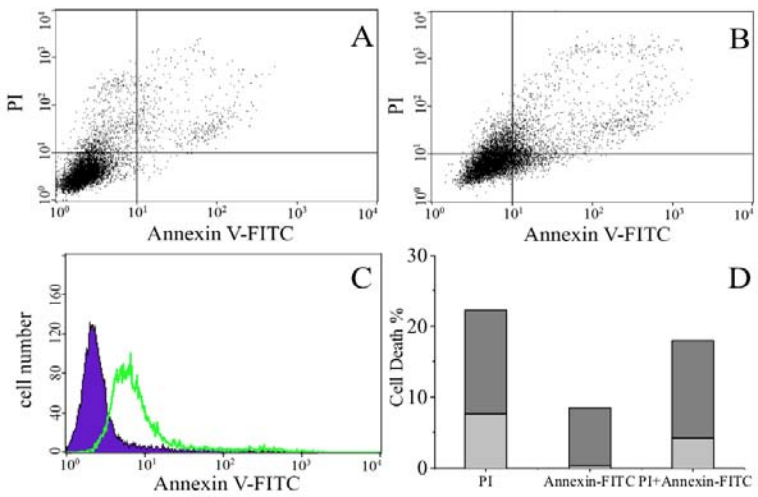


**Figure 5:** X-ray irradiated HeLa cells with (A) and without incubation (B) with PEG-CPP modified gold nanoparticles. Cells are scored for annexin V/PI double staining to determine the relative amount of live cells (bottom left), early apoptotic cells (bottom right), necrotic cells (top left) and late apoptotic cells (top right), respectively. (C) Enhanced Annexin V fluorescence staining in X-ray exposed cells treated with CPP-PEG modified gold nanoparticles (green line) or control (blue curve). (D) Percentage of cell death due to apoptosis alone (Annexin V-FITC), necrosis (PI) or late stage apoptosis (Annexin V-FITC and PI) in irradiated cells (light gray bar) or irradiated cells with PEG-CPP-Au nanoparticles (dark gray bar).

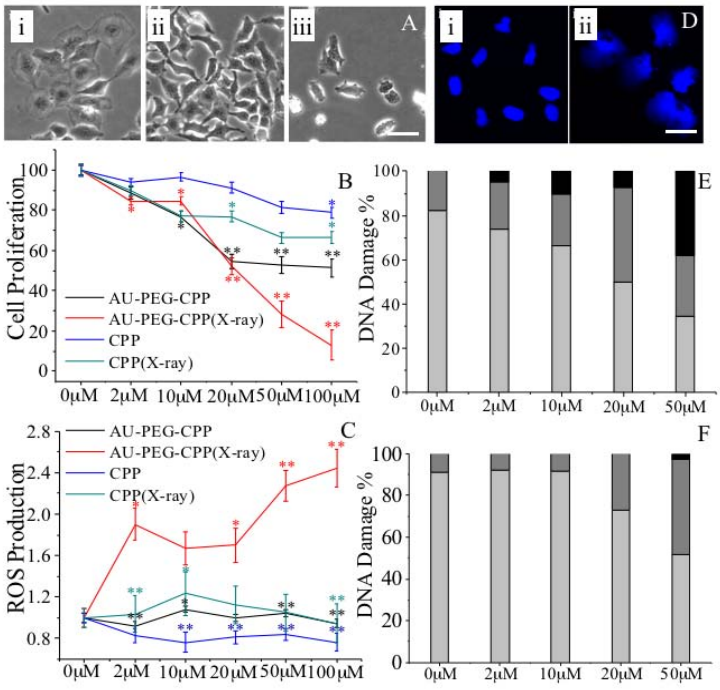


**Figure 6:** Concentration dependent killing of HeLa cells. Cells with i) no treatment, ii) X-ray irradiated, iii) treated with 50 μM PEG-CPP modified nanoparticles and X-ray radiation after 72 hours (A). The percentage of cells relative to the X-ray irradiated control after treatment with 2, 10, 20, 50 and 100 μM of PEG-CPP modified gold nanoparticles or CPP control 24 hours after X-ray irradiation (B). The relative amount of ROS produced using carboxy-$H_2$DCFDA assay compared to X-ray irradiated control after cells were treated with 2, 10, 20, 50 and 100 μM of PEG-CPP modified gold nanoparticles or CPP controls 1 hour after X-ray irradiation (C). HeLa cells treated with 50 μM of PEG-CPP modified gold nanoparticles, X-ray irradiated and stained with DAPI (Dii) or X-ray irradiated untreated cells (Di). DNA damage 2 days after treated with 2, 10, 20 and 50 μM PEG-CPP modified gold nanoparticles without (E) or with (F) X-ray irradiation (Light grey bar: No DNA damage, Grey bar: Moderate DNA damage, Black bar: Severe DNA damage). Scale bar is 20 μm. *, $P < 0.005$, **, $P < 0.001$.

PEG-CPP modified gold nanoparticles at 2, 10, 20, 50 and 100 μM were used to determine the optimal concentration required to kill a significant amount of cells after X-ray irradiation. Bright field microscopy image (Figure 6Aiii) showed a significant amount of cells exhibiting an abnormal phenotype and appeared dying 72 hours after X-ray irradiation, as compared to untreated cells (Figure 6Ai) or cells irradiated with an X-ray (Figure 6Aii). Cell proliferation and viability were tested with an MTT assay. Upon treatment with 50 and 100 μM

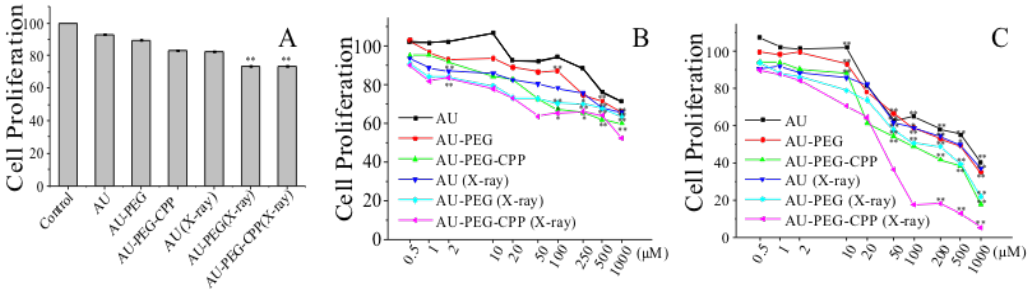


**Figure 7:** Fibroblast cells treated with 20 μM gold nanoparticles, PEG modified gold nanoparticles, or PEG-CPP modified gold nanoparticles. The percentage of cells relative to the untreated control after incubating with nanoparticles for 24 hours with X-ray irradiation or without X-ray irradiation (A). The percentage of live cells for different modified gold nanoparticles in normal fibroblast cells (B). The percentage of live cells for different modified gold nanoparticles in cancerous HeLa cells (C).

PEG-CPP gold nanoparticles and X-ray irradiated, only 28% and 12% survived, respectively (Figure 6B). This was in contrast with free CPP control at 50 and 100 μM concentrations, where 66% of cells survived when irradiated (Figure 6B). So, PEG-CPP modified nanoparticles showed a concentration dependent cytotoxicity to HeLa cells.

To determine if ROS generation was concentration dependent, HeLa cells were irradiated with 2, 10, 20, 50 and 100 μM of PEG-CPP modified gold nanoparticles. Figure 6C showed a 35.9 and 42.7 fold increase in ROS production at 50 and 100 μM concentrations. From Figure 6B and C, 50 μM of PEG-CPP modified nanoparticles seemed to be the optimum concentration to kill cells.

To strengthen this idea, the nuclei of cells treated with various concentrations of PEG-CPP modified gold nanoparticles were stained with DAPI two days after irradiation. Figure 6Dii showed that when cells were treated with 50 μM of PEG-CPP gold nanoparticles and were irradiated, the nuclei of cells were severely damaged, while DNA damage was less severe in irradiated but untreated cells (Figure 6Di). In addition, 37.9% of cells were severely damaged when cells were treated with 50 μM of PEG-CPP modified gold nanoparticles and were irradiated, compared to 7.1% of cells when incubated with 20 μM of PEG-CPP modified gold nanoparticles (Figure 6E). If there was no irradiation, only 2.4% of cells suffered from severe DNA damaged at 50 μM of PEG-CPP modified gold nanoparticles, while none was observed at a lower concentration (Figure 6F). Interestingly, 45.6% of cells had moderate DNA damage at 50 μM nanoparticle concentrations. Taken together, 50 μM of PEG-CPP modified gold nanoparticles was the optimal concentration to kill a significant number of HeLa cells at the concentrations tested.

### Cytotoxicity of PEG-CPP modified gold nanoparticles on fibroblast cells

Nanoparticles are known to internalize more easily into cancer cells than normal healthy cells. This makes them an ideal candidate in cancer treatment as they can destroy cancer tumors with minimal damage to healthy tissues. To test this hypothesis, normal healthy human fibroblast cells were treated with 20 μM of gold nanoparticles, PEG modified gold nanoparticles, and PEG-CPP modified gold nanoparticles, and their viabilities were measured using MTT assays. In contrast to cancer cells (Figure 2C and D), Figure 7A shows that only 26.83% of the fibroblast cells treated with PEG-CPP modified nanoparticles that underwent irradiation died. To determine the $IC_{50}$ values, cells were treated with different modified gold nanoparticles at concentrations ranging from 0.5 to 1000 μM for both fibroblast (B) and HeLa (C) cells. Based on MTT results, the $IC_{50}$ concentration of nanoparticles for HeLa cells were derived. No $IC_{50}$ values were obtained using fibroblast cells as 50% cell death relative to the control was not achieved even at 1000 μM for all the tested treatments (Figure 7B). The $IC_{50}$ values of gold nanoparticles, PEG modified gold nanoparticles, and PEG-CPP modified gold nanoparticles were determined to be 591, 353 and 94 μM without X-ray irradiation and 420, 127 and 23 μM with X-ray irradiation for HeLa cells, respectively.

## Conclusions

CPP-PEG-modified nanoparticles were incubated with either HeLa cells or normal human fibroblast cells and exposed to X-ray irradiation. Gold nanoparticles and PEG-modified gold nanoparticles were used as comparisons. PEG-CPP-Au nanoparticles were more effective in killing HeLa cells after X-ray irradiation when compared to Au or PEG-Au nanoparticles. One of the reasons might be the PEG-CPP-Au nanoparticles generated more intra-cellular reactive oxygen species in HeLa cells after X-ray irradiation than Au or PEG-Au nanoparticles. In addition, addition of free CPP with unmodified gold nanoparticles exhibit minimal cytotoxicity over the concentration range tested. This indicates that CPP by itself is not highly toxic to cancer cells. Also, PEG-CPP-Au nanoparticles can enhance the generation of free radical species to efficiently damage the DNA of cancerous HeLa cells. Interestingly, PEG-CPP modified gold nanoparticles generated a less severe cell proliferation effect on normal fibroblast cells than cancer cells. This might be because normal cells have been known to uptake nanoparticles inefficiently [45]. Taken together, our results indicated that the PEG-CPP-Au nanoparticles enhance the killing of cancer cells by generating more free radical species and caused DNA damage when cancer cells pre-incubated with PEG-CPP-Au nanoparticles were exposed to X-ray irradiation.

## Acknowledgement

This project was supported by a Director's New Innovator Award from the National Institute of Health (1DP2EB016572).

### References

1. Her, Jaffray DA, Allen C. Gold nanoparticles for applications in cancer radiotherapy: Mechanisms and recent advancements. Adv Drug Deliv Rev. 2015.

2. Jaffray DA. Image-guided radiotherapy: from current concept to future perspectives. Nat Rev Clin Oncol. 2012; 9: 688-699.

3. Barnett GC, West CM, Dunning AM, Elliott RM, Coles CE, Pharoah PD, et al. Normal tissue reactions to radiotherapy: towards tailoring treatment dose by genotype. Nat Rev Cancer. 2009; 9: 134-142.

4. Garrison JC, Uyeki EM. The effects of gamma radiation on chondrogenic development *in vitro*. Radiat Res. 1988; 116: 356-363.

5. Huang X, Jain PK, El-Sayed IH, El-Sayed MA. Gold nanoparticles: interesting optical properties and recent applications in cancer diagnostics and therapy. Nanomedicine (Lond). 2007; 2: 681-693.

6. Hainfeld JF, Slatkin DN, Smilowitz HM. The use of gold nanoparticles to enhance radiotherapy in mice. Phys Med Biol. 2004; 49: 309-315.

7. Huang X, Jain PK, El-Sayed IH, El-Sayed MA. Plasmonic photothermal therapy (PPTT) using gold nanoparticles. Lasers Med Sci. 2008; 23: 217-228.

8. Cooper DR, Bekah D, Nadeau JL. Gold nanoparticles and their alternatives for radiation therapy enhancement. Front Chem. 2014; 2: 86.

9. Kobayashi K, Usami N, Porcel E, Lacombe S, Le Sech C. Enhancement of radiation effect by heavy elements. Mutat Res. 2010; 704: 123-131.

10. Zhang P, Qiao Y, Wang C, Ma L, Su M. Enhanced radiation therapy with internalized polyelectrolyte modified nanoparticles. Nanoscale. 2014; 6: 10095-10099.

11. Zhang P, Qiao Y, Xia J, Guan J, Ma L, Su M. Enhanced radiation therapy with multilayer microdisks containing radiosensitizing gold nanoparticles. ACS Appl Mater Interfaces. 2015; 7: 4518-4524.

12. Prokop A, Davidson JM . Nanovehicular intracellular delivery systems. J Pharm Sci. 2008; 97: 3518-3590.

13. Kamaly N, Xiao Z, Valencia PM, Radovic-Moreno AF, Farokhzad OC. Targeted polymeric therapeutic nanoparticles: design, development and clinical translation. Chem Soc Rev. 2012; 41: 2971-3010.

14. Mayya KS, Schoeler B, Caruso F. Preparation and organization of nanoscale polyelectrolyte-coated gold nanoparticles. Adv Funct Mater. 2003; 13: 183-188.

15. Dizaj SM, Jafari S, Khosroushahi AY. A sight on the current nanoparticle-based gene delivery vectors. Nanoscale Res Lett. 2014; 9: 252.

16. Mieszawska AJ, Mulder WJ, Fayad ZA, Cormode DP. Multifunctional gold nanoparticles for diagnosis and therapy of disease. Mol Pharm. 2013; 10: 831-847.

17. Oh E, Delehanty JB, Sapsford KE, Susumu K, Goswami R, Blanco-Canosa JB, et al. Cellular uptake and fate of PEGylated gold nanoparticles is dependent on both cell-penetration peptides and particle size. ACS Nano. 2011; 5: 6434-6448.

18. Peer D, Karp JM, Hong S, Farokhzad OC, Margalit R, Langer R. Nanocarriers as an emerging platform for cancer therapy. Nat Nanotechnol. 2007; 2: 751-760.

19. Ghosh P, Han G, De M, Kim CK, Rotello VM . Gold nanoparticles in delivery applications. Adv Drug Deliv Rev. 2008; 60: 1307-1315.

20. Jain S, Hirst DG, O'Sullivan JM. Gold nanoparticles as novel agents for cancer therapy. Br J Radiol. 2012; 85: 101-113.

21. Kavosi B, Salimi A, Hallai R, Moradi F. Ultrasensitive electrochemical immunosensor for PSA biomarker detection in prostate cancer cells using gold nanoparticles/PAMAM dendrimer loaded with enzyme linked aptamer as integrated triple signal amplification strategy. Biosens Bioelectron. 2015; 74: 915-923.

22. Larguinho M, Canto R, Cordeiro M, Pedrosa P, Fortuna A, Vinhas R, et al. Gold nanoprobe-based non-crosslinking hybridization for molecular diagnostics. Expert Rev Mol Diagn. 2015; 15: 1355-1368.

23. Oh E, Susumu K, Goswami R, Mattoussi H. One-phase synthesis of water-soluble gold nanoparticles with control over size and surface functionalities. Langmuir. 2010; 26: 7604-7613.

24. Ajith TA. Strategies used in the clinical trials of gene therapy for cancer. J Exp Ther Oncol. 2015; 11: 33-39.

25. Cruje C, Yang C, Uertz J, Van Prooijen M, Chithrani BD. Optimization of PEG coated nanoscale gold particles for enhanced radiation therapy. RSC Adv. 2015; 5: 101525-101532.

26. Margus H, Padari K, Pooga M. Cell-penetrating peptides as versatile vehicles for oligonucleotide delivery. Mol Ther. 2012; 20: 525-533.

27. Lin YX, Gao YJ, Wang Y, Qiao ZY, Fan G, Qiao SL, et al. pH-sensitive polymeric nanoparticles with gold (I) compound payloads synergistically induce cancer cell death through modulation of autophagy. Mol Pharm. 2015; 12: 2869-2878.

28. Zhang XD, Wu D, Shen X, Chen J, Sun YM, Liu PX, Liang XJ. Size-dependent radiosensitization of PEG-coated gold nanoparticles for cancer radiation therapy. Biomaterials. 2012; 33: 6408-6419.

29. Mackay JA, Szoka FC Jr. HIV TAT Protein Transduction Domain Mediated Cell Binding and Intracellular Delivery of Nanoparticles. J Dispers Sci Technol. 2003; 24: 465-473.

30. Schuemann J, Berbeco R, Chithrani DB, Cho SH, Kumar R, McMahon SJ, et al. Roadmap to Clinical Use of Gold Nanoparticles for Radiation Sensitization. Int J Radiat Oncol Biol Phys. 2016; 94: 189-205.

31. Halliwell B. Effect of diet on cancer development: is oxidative DNA damage a biomarker? Free Radic Biol Med. 2002; 32: 968-974.

32. Klaunig JE, Kamendulis LM, Hocevar BA. Oxidative stress and oxidative damage in carcinogenesis. Toxicol Pathol. 2010; 38: 96-109.

33. Riley PA. Free radicals in biology: oxidative stress and the effects of ionizing radiation. Int J Radiat Biol. 1994; 65: 27-33.

34. Weiss JF. Pharmacologic approaches to protection against radiation-induced lethality and other damage. Environ Health Perspectives. 1997; 105: 1473.

35. Kalpana KB, Devipriya N, Srinivasan M, Menon VP. Investigation of the radioprotective efficacy of hesperidin against gamma-radiation induced cellular damage in cultured human peripheral blood lymphocytes. Mutat Res. 2009; 676: 54-61.

36. Zhang YJ, Guo J, Qi YH, Shao QJ, Liang J. The prevention of radiation-induced DNA damage and apoptosis in human intestinal epithelial cells by salvianic acid A. J Radiat Res Appl Sci. 2014; 7: 274-285.

37. Kang MA, So EY, Simons AL, Spitz DR, Ouchi T. DNA damage induces reactive oxygen species generation through the H2AX-Nox1/Rac1 pathway. Cell Death Dis. 2012; 3: e249.

38. Kim DA, Suh EK. Defying DNA double-strand break-induced death during prophase I meiosis by temporal TAp63a phosphorylation regulation in developing mouse oocytes. Mol Cell Biol. 2014; 34: 1460-1473.

39. Polci R, Peng A, Chen PL, Riley DJ, Chen Y. NIMA-related protein kinase 1 is involved early in the ionizing radiation-induced DNA damage response. Cancer Res. 2004; 64: 8800-8803.

40. Podhorecka M, Skladanowski A, Bozko P. H2AX Phosphorylation: Its Role in DNA Damage Response and Cancer Therapy. J Nucleic Acids. 2010; 2010.

41. Kang MA, So EY, Simons AL, Spitz DR, Ouchi T. DNA damage induces reactive oxygen species generation through the H2AX-Nox1/Rac1 pathway. Cell Death Dis. 2012; 3: e249.

42. Liang SH, Clarke MF. Regulation of p53 localization. Eur J Biochem. 2001; 268: 2779-2783.

43. Sherr CJ. Principles of tumor suppression. Cell. 2004; 116: 235-246.

44. Yumita N, Iwase Y, Nishi K, Komatsu H, Takeda K, Onodera K, et al. Involvement of reactive oxygen species in sonodynamically induced apoptosis using a novel porphyrin derivative. Theranostics. 2012; 2: 880-888.

45. Kong T, Zeng J, Wang X, Yang X, Yang Y, McQuarrie S, et al. Enhancement of radiation cytotoxicity in breast-cancer cells by localized attachment of gold nanoparticles. Small. 2008; 4: 1537-1543.